

Barium titanate nanoparticle self-organization in an external electric field

Christine Lausser,^a Dirk Zahn^b and Helmut Cölfen^{†*a}

We describe the formation of BaTiO₃ superstructures from precursor nanoparticles and the use of ferroelectric properties to trigger a hierarchical growth mechanism. Without specific treatment, the precursor nanoparticles comprise of ferroelectric domains that are oriented randomly (domains of the same spontaneous polarisation). However, using an external electric field the ferroelectric polarization of all domains can be oriented into the same direction and an enduring microscopic dipole results for each precursor nanoparticle. Self-organization of the polarized BaTiO₃ nanoparticles to dumbbell- and cross-shaped superstructures was observed as a combined result of nanoparticle alignment by the electric field and crystallographic fusion of the nanoparticles under defined coincidence angles following an oriented attachment process. These structures were characterized by electron microscopy and the nanoparticle superstructure formation guided by electrical dipole fields is explained by molecular modeling. The combination of an orienting physical field with the crystallographic lock in dictated by the crystal lattice is a new mechanism for the guided self-organization of nanoparticles.

Introduction

Controlled self-organisation of nanoparticles can lead to new materials and bottom up approaches are a very promising and important strategy in materials synthesis. In this respect, mesocrystals receive increasing attention of chemists and physicists. A mesocrystal is defined as a superstructure of crystalline nanoparticles with mutual orientation between the nanocrystal building units.¹⁻⁴ The crystalline subunits are very often found in perfect mutual 3D order, but sometimes, the mutual order can be different and for example follow field lines of a physical field. Several different mechanisms were reported for the formation of mesocrystals in the recent years.² One of them is the nanoparticle orientation by means of external physical forces. The ordering physical forces like dipole,⁵ magnetic⁶ or electric forces^{5,7} as well as polarization forces have to be anisotropic to permit an ordered arrangement of nanoparticles. On the other hand, the nanoparticles have to be anisotropic with respect to their interaction potentials with the physical field for their alignment. This anisotropy could be oppositely charged counter faces of a crystal, a dipole or magnetic moment along one nanocrystal axis or differences in the polarizability along different crystallographic directions.

Intrinsic electric field lines around a fluorapatite mesocrystal seed generated in a gelatin matrix could be demonstrated by Kniep and co-workers by electron holography pointing out the importance of the organic component, which represents aligned dipoles in the form of gelatin triple helices in this case.⁵ However, external electric fields can also be used to create 2D and 3D self-organized superstructures as it was demonstrated for CdS and CdSe nanorods, which exhibit a permanent electric dipole in their crystal structure.⁷⁻⁹ In the present report, we worked with ferroelectric nanoparticles of barium titanate (BaTiO₃). Ferroelectric materials feature spontaneous electric polarization that can be switched to symmetry equivalent states with an external electric field.¹⁰ The obtained polarization of the particles remains after removing the external electric field. This makes BaTiO₃ nanoparticles excellent candidates to orient them to superstructures using external electric fields. In addition, BaTiO₃ is insoluble in water and ethanol and thus, no shielding of the electrical field by ions in solution takes place. The insolubility also ensures that all observed structures are nanoparticle superstructures and not formed *via* dissolution–recrystallization.

Ferroelectric ABO₃ perovskites are not only of fundamental interest but also of technological importance due to the strong coupling of their polarization with electric and stress fields. The property of switchable polarization with an external applied electric field makes them useful for non-volatile memories and micro-electromechanical systems. Other possible applications could be the fabrication of multilayer capacitors or piezoelectric transducers.^{11,12} In this report we demonstrate the ordered self-organization of BaTiO₃ nanoparticles to superstructures after polarization of the particles in an external electric field combined with oriented nanoparticle attachment and crystallographic

^aMax-Planck-Institute of Colloids and Interfaces, Colloid Chemistry, Research Campus Golm, Am Mühlenberg, D-14424 Potsdam, Germany. E-mail: helmut.coelfen@uni-konstanz.de

^bFriedrich-Alexander University of Erlangen-Nürnberg, Computer Chemistry Center, Nägelsbachstraße 25, 91052 Erlangen, Germany

[†] Present address: University of Konstanz, Physical Chemistry, Universitätsstr. 10, D-78457 Konstanz, Germany.

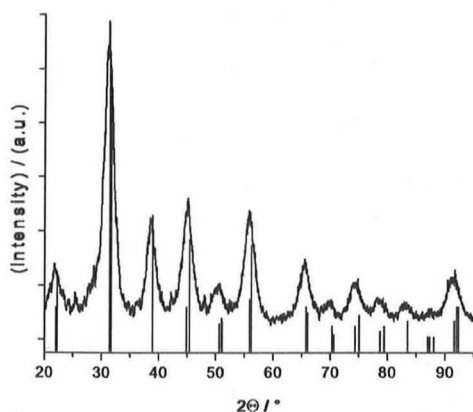


Fig. 1 Wide angle X-ray diffraction results on the BaTiO₃ nanoparticles demonstrating the tetragonal ferroelectric phase. The thin lines are the reference peaks for the tetragonal phase.

fusion at defined coincidence angles. This is a new mechanism for nanoparticle self-organization and synthesis of nanostructured materials.

Results and discussion

The prepared BaTiO₃ nanoparticles were obtained in the ferroelectric tetragonal BaTiO₃ phase as demonstrated by WAXS (Fig. 1).

Without an electric field, no interaction between the BaTiO₃ nanoparticles can be observed. After exposing a BaTiO₃-dispersion with sizes <50 nm to a homogeneous electric field of 10⁵ V m⁻¹ field strength for 7 h, nanoparticle self-organization was monitored once the sample was removed from the external electric field. The nanoparticles were observed to form superstructures with cross-like and dumbbell morphologies on the glass-slide after drying of the substrate as shown in Fig. 2.

The ferroelectric domains within the BaTiO₃ are mutually oriented by the external electric field. Thus, the nanoparticles are polarized and form microscopic dipoles. Since BaTiO₃ is piezoelectric as well, the particles are deformed mechanically by the electric field. Thereby an extension of the crystalline structure is assumed, the polarized faces increase and the particles can be oriented easily.

The arrangement is expected to follow nanoparticle orientation by the electric field with subsequent oriented attachment



Fig. 3 Schematic illustration of the oriented attachment of the dipolar nanoparticles.

mechanism.¹³ This process can take place when nanoparticles attach to each other *via* a high-energy face with a match of the crystal lattice. Crystallographic fusion of the two high-energy faces results in energy gain. This phenomenon was first described by Banfield *et al.* for the appearance of iron hydroxide as the product of biomineralization¹³ and is nowadays known for a number of systems.^{14–19} In our case, the particles in the dispersion can collide with each other due to the random Brownian motion whilst oriented attractive forces result from the dipolar particle character. On the surface of the particles there is some benzyl alcohol as determined by Fourier transform spectroscopy. It was used in the syntheses of the particles as a stabilizer and inhibits the particles to fuse immediately.

The growth of the nanoparticle superstructure is expected to begin as an elongated dipole. Few dipolar nanoparticles fuse and build up the seed as illustrated in Fig. 3. Due to the oriented attachment, the seed grows in length and thus the electric field, based on generated accumulated dipoles, increases. At a later growth stage, further parallel attachment of the particles is replaced by branching. This may be rationalized by the alignment of dipolar nanoparticles according to the electric field lines of the seed particle. Hence, branching of the seed is initiated where the field strength is largest, *i.e.* at the poles, and a dumbbell-like shaped polycrystal results as the mature seed.⁵ This picture implies that the free dipolar particles in the dispersion arrange according to the electric field during association to the seed. However, despite fusion of the particles, no ripening into a classical single crystal with well developed faces takes place as is demonstrated with TEM measurements. It is obvious that the crystals are made by smaller particles as one can see in Fig. 4b.

The particles arrange primarily along the main field lines of the initial dipole so that they aggregate to rod-like superstructures (marked with white lines in Fig. 4b). However, the electron diffraction shows a ring-like pattern, which is typical for polycrystalline materials. Since obviously a mutual arrangement of most of the nanoparticles exists, this phenomenon can be explained by a small fraction of non-polarised particles. This

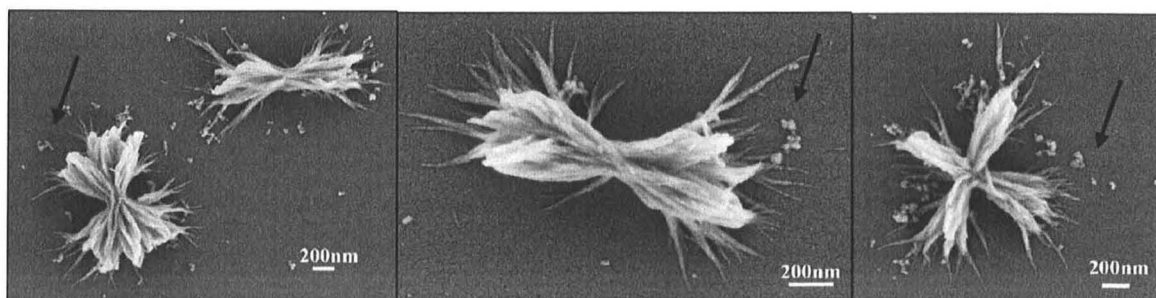


Fig. 2 SEM images of the BaTiO₃ crystals synthesized by means of an external electric field. Dumbbell-like (left and middle) and cross-shaped crystals are formed by aggregation of nanoparticles (marked with arrows).

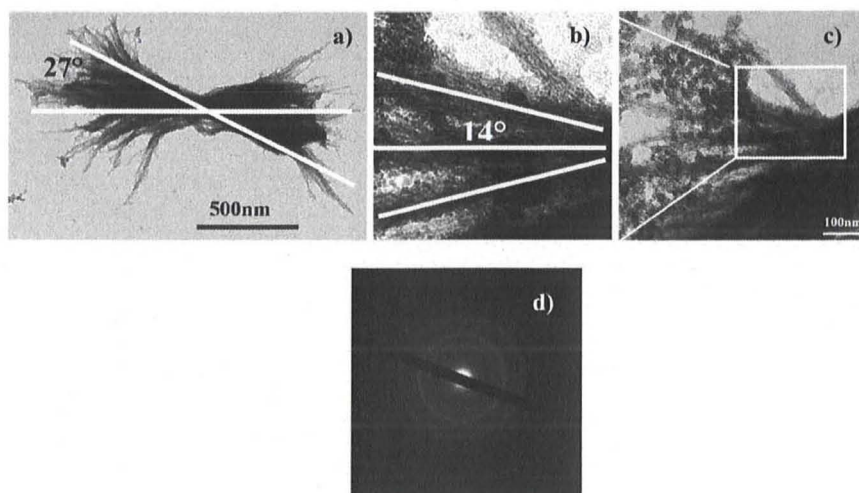


Fig. 4 TEM images of BaTiO₃ crystals grown by means of an external electric field. (a) The dumbbells are built up by smaller particles. (b) and (c) The particles organize each other and arrange themselves along the electric field lines (the arrangement is marked with white lines). (d) SAED shows a typical polycrystalline electron diffraction pattern.

fraction cannot be quantified with respect to the aligned nanoparticles since the latter cannot be recognized as individual nanoparticles anymore. The dispersion of nanoparticles was exposed to the external electric field only for limited time and not all particles might have been polarised or may have already lost their polarization before the nanoparticle superstructure gets fixed. This results in random orientation of these nanoparticles as shown in Fig. 4c. Another plausible reason for the non-oriented nanoparticles can be obtained when their size is measured. The critical size of barium titanate for ferroelectric properties was theoretically estimated in several reports to be 44 nm.^{20–22} Below that size the nanoparticles should exhibit no ferroelectric properties. However, some experiments demonstrated that the critical size of ferroelectric BaTiO₃ is between 10 and 100 nm depending on the method of fabrication.^{23,24} The size of the non-oriented nanoparticles is determined to be 3–7 nm which is below the

critical size for ferroelectricity in BaTiO₃ (see TEM Fig. 5). This agrees with the size of 4 nm determined *via* the Scherrer equation from Fig. 1.

The starting point for the formation of the cross-like morphologies is a dipole. The association of further dipolar particles reflects a compromise between electric field energy and favorable interface arrangement, which is dictated by the crystal lattice. For small dipoles the electric field is too weak to compensate the interface energy needed for branching. However, with increasing size of the primary dipole, additional particles are preferentially coordinated along the field lines as schematically shown in Fig. 6.

At this growth stage, further polarised particles experience significant electrostatic attraction, and branching of the primary dipole becomes possible. The observed angles (see also Fig. 4) tend to follow the rules for grain boundary angles with

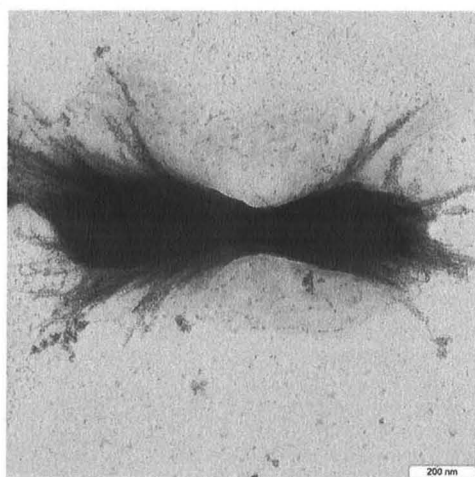


Fig. 5 TEM images of a BaTiO₃ nanoparticle superstructure grown by means of an external electric field. Non-aligned 3–7 nm big nanoparticles can be detected in the surrounding.

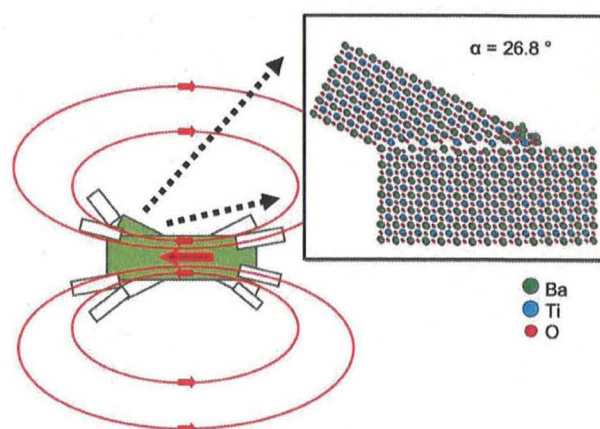


Fig. 6 Left: electric field lines of a dipole. Polarised nanoparticles are aligned according to the electric field lines, but respecting discrete tilting angles as given by the requirement of interfaces with coherent lattice sites. Right: molecular simulation model demonstrating the stability of favorable grain boundary arrangements (shown for 26.8°) based on coincidence lattice site angles.

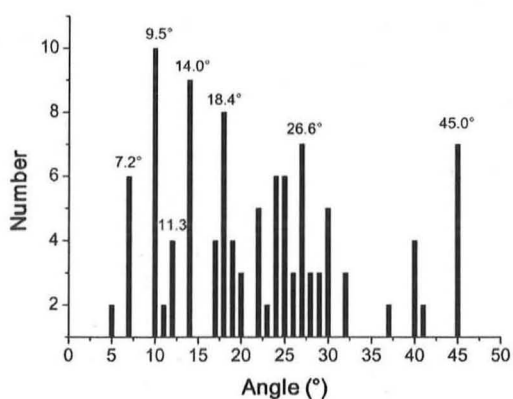


Fig. 7 Grain boundary angles for 119 BaTiO₃ nanoparticle grain boundaries. The labelled angles are those with coincidence lattice sites which are preferred orientations for crystallographic lock in.

coincidence lattice sites, that is $\alpha = \tan^{-1}(1/n)$ with $n = 1, 2, 3, \dots$ and thus $\alpha = 45^\circ, 26.6^\circ, 18.4^\circ, 14.0^\circ, 11.3^\circ, 9.5^\circ, 7.2^\circ, \dots, 0^\circ$. This argument is supported by Fig. 7 from which experimentally determined preferred grain boundary angles can be seen clearly. For these preferred angles, crystallographic fusion of the nanoparticles to minimize the surface energy is possible. This fixes the mutual nanoparticle orientation, and the disintegration of the nanoparticle superstructures after the nanoparticle polarization has disappeared is prevented. This is indeed observed.

To confirm the intuitive picture of branching at angles that allow coincidence lattice sites, we prepared an atomistic model comprising of two BaTiO₃ blocks that are associated at a tilting angle of 26.8° (which reflects the tilting angle of the cross-like structures as illustrated in Fig. 4a). Structural relaxation as obtained from molecular dynamics simulations at room temperature reveals the close interplay of coinciding crystal motifs and small lattice distortion at the interface of both BaTiO₃ blocks. Angles that do not allow for the coherent matching of lattice sites lead to disordered interfaces which are penalized by the potential energy.

Indeed, large distortion is only observed for the onset of branching (Fig. 6, right). A full characterization of all possible interface arrangements of BaTiO₃ blocks and the assessment of the underlying interface energies exceed the scope of the present study. However, from the combination of experimental findings and modelling results we suggest the competition of the meso-scale electric field and the association of polarized BaTiO₃ blocks at favourable tilting angles as the growth mechanism leading to the observed cross-like/dumbbell morphologies.

Conclusion

In summary, we have shown that ferroelectric BaTiO₃ nanoparticles can be arranged to superstructures by pre-treating the dispersion by an external electric field of 1 kV for several hours. Due to their ferroelectric character the particles got polarized and retain the polarization after removing the electric field. The arrangement of the particles is governed by a competition of electric field and favorable interface energy and thus by a combined action of nanoparticle alignment in an external

physical field and oriented attachment at favourable angles for crystal lattice matching. First, parallel attachment leads to prismatic seeds of large dipole moment as compared to the primary nanoparticles. The resulting dipole field then induces the rearrangement of further primary nanoparticles and thus a change of the seed's growth mechanism in favor of dumbbell and cross-like morphologies. The combination of alignment by an external field with crystallographic lock in at preferred orientations dictated by the crystal lattice is a novel mechanism for the defined self-organization of nanoparticles. It should be in principle transferable to other physical fields like magnetic fields and is an exciting possibility for the generation of nanostructured materials.

Materials and methods

Barium titanate nanoparticles were prepared according to a protocol described by Niederberger *et al.*²⁵ All procedures were carried out in a glove box. Ba (2 mmol) was stirred in a vial with 25 mL benzyl alcohol at slightly elevated temperature (*ca.* 40–50 °C). As soon as it was completely dissolved 1 mmol equivalent of Ti(OiPr) was added. After stirring for a few minutes the reaction mixture was transferred into an autoclave and heated for 48 h at 200 °C.

The formed nanoparticles were kept in absolute ethanol. Since after a while aggregation occurs, nanoparticles ≤ 50 nm were separated from the aggregates by means of preparative ultracentrifugation (Beckman L70 ultracentrifuge, Beckman SW32 rotor), for 10 min at 20 000 rpm at 25 °C. The supernatant was highly diluted (*ca.* 1 : 100) in order to avoid re-aggregation.

For the subsequent electric field driven alignment experiments, we used the cell shown below. The plastic box is effused by epoxy resin and contains a quartz cuvette with a cross-section area of 1 cm². On the right- and left-hand of the cuvette there are electrodes of copper, which can be connected to a high voltage power supply. In order to put the BaTiO₃ dispersion into the cell, and consequently into the electric field, a glass-spoon (Fig. 8b) was employed.

A glass-slide and a TEM-grid of copper covered by carbon, deposited on the spoon, were placed into the cuvette. After filling 1 mL of the BaTiO₃ nanoparticle dispersion into the vessel, the

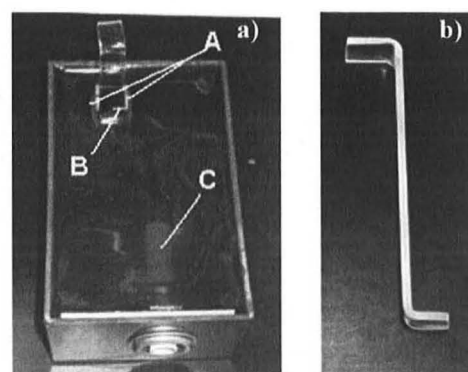


Fig. 8 (a) The cell used for the experiments: A: copper-electrodes, B: quartz cuvette; C: connection to high-voltage power supply. (b) Glass-spoon.

cell was connected to a voltage of 1 kV for 7 hours. Subsequently the glass-spoon was carefully taken out together with the glass-slide and the TEM-grid. The rest of the ethanol was able to evaporate in air while the spoon was standing in a beaker.

The microstructure of the resulting crystals was observed by a scanning electron microscope (SEM) LEO 1550-Gemini-System. The transmission electron microscope (TEM) images were recorded on a Zeiss EM912 Ω microscope operated at 120 kV.

Molecular modelling

The molecular simulation studies were based on the force-field model of Tinte *et al.*²⁶ This interaction potential was based on first-principles calculations and demonstrated to accurately reproduce a series of structural and thermodynamic properties, including the phase diagram. Two rectangular prisms were cut from the single crystal, tilted by 26.8° and merged. Overlapping atoms were cut and the resulting model of 936 formulae units was carefully relaxed. Along this line, we first performed a steepest-descent energy minimization to amend unfavourable local arrangements and optimize the placement of the 'ongrown' block of BaTiO₃. After adjustment of the distance and location along the lower block surface, further relaxation of the system was explored from a 100 ps molecular dynamics run using a simulation time step of 1 fs and explicit summation of all interaction forces without cut-off-criteria.

Acknowledgements

We thank Rona Pitschke and Heike Runge for SEM- and TEM-measurements and the Max-Planck-Society for financial support. The authors also thank Markus Niederberger for preparing the BaTiO₃ nanoparticles used in the experiments. Dr Jong Seto is acknowledged for analysis of the WAXS diffractogram.

References

- 1 H. Cölfen and M. Antonietti, *Angew. Chem., Int. Ed.*, 2005, **44**, 5576–5591.
- 2 R. Q. Song and H. Cölfen, *Adv. Mater.*, 2009, **21**, 1–30.
- 3 L. Zhou and P. O'Brien, *Small*, 2008, **4**, 1566–1574.
- 4 H. Cölfen and M. Antonietti, *Mesocrystals and Nonclassical Crystallization*, John Wiley & Sons, 2008.
- 5 P. Simon, D. Zahn, H. Lichte and M. Kniep, *Angew. Chem., Int. Ed.*, 2006, **45**, 1911–1915.
- 6 S. Q. Li, C. Y. Wu, K. Sassa and S. Asai, *Mater. Sci. Eng., A*, 2006, **422**, 227–231.
- 7 K. M. Ryan, A. Mastroianni, K. A. Stancil, H. T. Liu and A. P. Alivisatos, *Nano Lett.*, 2006, **6**, 1479–1482.
- 8 L. Carbone, C. Nobile, M. De Giorg, F. D. Sala, G. Morello, P. Pompa, M. Hytch, E. Snoeck, A. Fiore, I. R. Franchini, M. Nadasan, A. F. Silvestre, L. Chiodo, S. Kudera, R. Cingolani, R. Krahne and L. Manna, *Nano Lett.*, 2007, **7**, 2942–2950.
- 9 C. Querner, M. D. Fischbein, P. A. Heiney and M. Drndic, *Adv. Mater.*, 2008, **20**, 2308.
- 10 R. V. K. Mangalam, N. Ray, U. V. Waghmare, A. Sundaresan and C. N. R. Rao, *Solid State Commun.*, 2009, **149**, 1–5.
- 11 A. S. Bhalla, R. Y. Guo and R. Roy, *Mater. Res. Innovations*, 2000, **4**, 3–26.
- 12 N. Setter, D. Damjanovic, L. Eng, G. Fox, S. Gevorgian, S. Hong, A. Kingon, H. Kohlstedt, N. Y. Park, G. B. Stephenson, I. Stolitchnov, A. K. Taganstev, D. V. Taylor, T. Yamada and S. Streiffer, *J. Appl. Phys.*, 2006, **100**, 051606.
- 13 J. F. Banfield, S. A. Welch, H. Z. Zhang, T. T. Ebert and R. L. Penn, *Science*, 2000, **289**, 751–754.
- 14 M. Antonietti, M. Niederberger and B. Smarsly, *Dalton Trans.*, 2008, 18–24.
- 15 N. M. Kinsinger, A. Wong, D. S. Li, F. Villalobos and D. Kisailus, *Cryst. Growth Des.*, 2010, **10**, 5254–5261.
- 16 M. Niederberger and H. Cölfen, *Phys. Chem. Chem. Phys.*, 2006, **8**, 3271–3287.
- 17 J. J. Ning, K. K. Men, G. J. Xiao, B. Zou, L. Wang, Q. Q. Dai, B. B. Liu and G. T. Zou, *CrystEngComm*, 2010, **12**, 4275–4279.
- 18 R. L. Penn, *J. Phys. Chem. B*, 2004, **108**, 12707–12712.
- 19 Q. Zhang, S. J. Liu and S. H. Yu, *J. Mater. Chem.*, 2009, **19**, 191–207.
- 20 S. Lin, T. Lu, C. Q. Jin and X. H. Wang, *Phys. Rev. B: Condens. Matter Mater. Phys.*, 2006, **74**, 134115.
- 21 Y. X. Wang, W. L. Zhong, C. L. Wang, P. L. Zhang and X. T. Su, *Chin. Phys.*, 2002, **11**, 714–719.
- 22 W. L. Zhong, Y. G. Wang, P. L. Zhang and B. D. Qu, *Phys. Rev. B: Condens. Matter Mater. Phys.*, 1994, **50**, 698–703.
- 23 C. J. Xiao, Z. H. Chi, F. Y. Li, S. M. Feng, C. Q. Jin, X. H. Wang, X. Y. Deng and L. T. Li, *Chin. Phys.*, 2007, **16**, 3125–3128.
- 24 Z. Zhao, V. Buscaglia, M. Viviani, M. T. Buscaglia, L. Mitoseriu, A. Testino, M. Nygren, M. Johnsson and P. Nanni, *Phys. Rev. B: Condens. Matter Mater. Phys.*, 2004, **70**, 024107.
- 25 M. Niederberger, N. Pinna, J. Polleux and M. Antonietti, *Angew. Chem., Int. Ed.*, 2004, **43**, 2270–2273.
- 26 S. Tinte, M. G. Stachiotti, M. Sepiarsky, R. L. Migoni and C. O. Rodriguez, *J. Phys.: Condens. Matter*, 1999, **11**, 9679.